

The Effect of Combination Anti-Endothelial Growth Factor Receptor and Anti-Vascular Endothelial Growth Factor Receptor 2 Targeted Therapy on Lymph Node Metastasis

A Study in an Orthotopic Nude Mouse Model of Squamous Cell Carcinoma of the Oral Tongue

Daisuke Sano, MD, PhD; Sungweon Choi, DDS, PhD; Zvonimir Luka Milas, MD; Ge Zhou, PhD; Chad E. Galer, MD; Ying-Wen Su, MD; Maria Gule, MD; Mei Zhao, MD; Zhenping Zhu, PhD; Jeffrey N. Myers, MD, PhD

Objective: To evaluate the therapeutic effect of treatment with a combination of the monoclonal antibodies to the vascular endothelial growth factor receptor (DC101) and the epidermal growth factor receptor (cetuximab) in an orthotopic nude mouse model of metastatic squamous cell carcinoma of the oral tongue (SCCOT).

Design: In vivo study.

Setting: A translational research laboratory at a comprehensive cancer center.

Subjects: Male athymic nude mice aged 8 to 12 weeks.

Intervention: To develop orthotopic nude mouse models of SCCOT, OSC-19 cells or luciferase (Luc)-expressing OSC-19-Luc and JMAR-Luc cells were injected into the tongues of nude mice. Animals were randomly divided into 4 groups: DC101 alone, cetuximab alone, DC101 plus cetuximab, or placebo, and all treatments were administered twice per week for 4 weeks. The in vivo antitumor activity was monitored noninvasively by bioluminescence imaging. Tumors were resected at necropsy, and immunohistochemical and immunofluorescent staining were performed.

Main Outcome Measures: Tumor size, bioluminescence, animal survival, and percentage of animals with lymph node metastasis.

Results: At the conclusion of the treatment period, the mean tumor volumes in the cetuximab alone and the DC101 plus cetuximab groups had decreased significantly compared with those that received the placebo control (68% [$P = .002$] and 84% [$P < .001$], respectively). Significant effects of the treatment were also observed in bioluminescence imaging. Mice treated with DC101 plus cetuximab also lived longer and had a lower incidence of neck lymph node metastases compared with the control group ($P = .003$).

Conclusions: Treatment with DC101 plus cetuximab inhibited the growth of SCCOT and decreased the incidence of the neck lymph node metastases in vivo. These results suggest that this combination treatment may be an effective strategy against metastatic SCCOT and warrants further preclinical trials.

Arch Otolaryngol Head Neck Surg. 2009;135(4):411-420

Author Affiliations:

Departments of Head and Neck Surgery (Drs Sano, Choi, Milas, Zhou, Galer, Su, Gule, Zhao, and Myers) and Cancer Biology (Dr Myers), The University of Texas M. D. Anderson Cancer Center, Houston; and ImClone Systems Inc, New York, New York (Dr Zhu).

ORAL CAVITY CANCER CONSISTENTLY ranks as one of the 10 most frequently diagnosed cancers in the world and account for 34 000 new diagnoses and 7500 deaths in 2007 in the United States.¹ Squamous cell carcinoma of the oral tongue (SCCOT) is the most common tumor of the oral cavity. Despite advances in surgery and radiation therapy, the 5-year survival rate for oral cancer has not improved significantly over the past several decades and remains at 50% to 55%.² This is primarily because patients continue to die from metastatic disease, despite some improve-

ment in local control. Although metastasis to cervical lymph nodes is the most reliable predictor of failure of SCCOT treatment,³ the cellular and molecular mechanisms of metastasis in SCCOT are poorly understood. Therefore, the development of new systemic adjuvant strategies for the treatment of the SCCOT primary tumor and its metastatic lesions is necessary to provide improved disease control and survival.

Extensive efforts have been made to develop targeted molecular therapies designed to inhibit key signaling pathways involved in tumor growth and dissemination to metastatic sites, and some prom-

ising results have been demonstrated in the use of these therapies against various malignant tumors in preclinical and clinical studies.⁴ Combining these targeted therapies with the goal of increasing efficacy and reducing the toxicity profile is a rapidly emerging therapeutic strategy. One such approach that is showing promise is combined inhibition of the vascular endothelial growth factor (VEGF) and the epidermal growth factor receptor (EGFR).⁵

VEGF signaling plays a key role in tumor angiogenesis, which is crucial for the progression and metastasis of many types of human cancers, including induction of endothelial cell proliferation, migration, survival, and capillary tube formation.⁶ Several studies have reported that overexpression of VEGF is associated with poor prognosis and metastases in SCCOT, since high VEGF and VEGFR expression correlate with regional lymph node metastases in SCCOT⁷⁻¹⁰ and its receptor (VEGFR) is up-regulated in tumor development in squamous cell carcinoma of the head and neck (SCCHN).¹¹ These findings suggest that the inhibition of angiogenic signaling is an intriguing potential therapeutic target in SCCOT.

The EGFR plays a key role in promoting cellular proliferation and survival.¹² Activation of the EGFR also regulates many processes associated with metastasis,¹³ and its ligand, EGF, has been shown to increase motility, in vitro invasion, and metastatic potential in several different tumor cells.¹⁴ Inhibitors of EGFR signaling have shown significant inhibition of tumor growth in numerous preclinical models.¹⁵⁻¹⁷ Overexpression of EGFR has ranged from 34% to 80% in SCCHN, and this overexpression is associated with poor disease control and decreased survival.^{18,19} Preclinical studies have provided evidence of the significant therapeutic effects of EGFR inhibitors in SCCHN.²⁰ Furthermore, Bonner et al²¹ showed that cetuximab, a monoclonal antibody to EGFR, with radiotherapy improved locoregional control and survival of patients with locoregionally advanced SCCHN compared with treatment with radiotherapy alone in a phase 3 clinical trial.

Despite the beneficial effects of cetuximab in the treatment of SCCHN, locoregional and distant failure rates remain high in the published clinical trials. Therefore, investigators are trying to identify ways to improve the results of treatment of SCCHN via EGFR inhibition. Some studies have reported the synergistic antitumor effects of a targeted therapy combining EGFR and VEGFR.⁵ In addition, clinical trials combining inhibitors of EGFR and VEGF are already showing promise in non-small cell lung cancer.²² Therefore, the inhibitory effect produced when these 2 signaling pathways are combined may result in greater antitumor outcomes against metastatic SCCOT than would be produced by either pathway alone.

Although we have studied the effect of inhibition against EGFR and VEGFR signaling with a small molecule tyrosine kinase inhibitor on an orthotopic nude mouse model of SCCOT,²⁰ we have not previously used antibodies to target the combination of EGFR and VEGFR-2. In the present study, we hypothesized that inhibition of the EGFR and VEGFR-2 signaling pathways using monoclonal antibodies to the 2 receptors would inhibit tumor growth and metastasis in an orthotopic nude mouse model of SCCOT. To test this hypothesis, we in-

vestigated the preclinical efficacy of DC101, an anti-mouse monoclonal VEGFR-2 antibody, alone and in combination with cetuximab, an anti-EGFR monoclonal antibody, against established invasive and metastatic SCCOT tumors in an orthotopic nude mice model using a bioluminescence image system.

METHODS

ANIMALS AND MAINTENANCE

Male athymic nude mice aged 8 to 12 weeks were purchased from the animal production area of the National Cancer Institute-Frederick Cancer Research and Development Center (Frederick, Maryland). In accordance with current regulations and standards of the US Department of Agriculture, the US Department of Health and Human Services, and the National Institutes of Health (NIH), the mice were housed and maintained in laminar flow cabinets under specific pathogen-free conditions in facilities approved by the American Association for Accreditation of Laboratory Animal Care. The mice were used in accordance with the Animal Care and Use Guidelines of M. D. Anderson Cancer Center under a protocol approved by the Institutional Animal Care Use Committee.

CELL LINES AND CULTURE CONDITIONS

For these studies, we used the invasive oral SCC cell line JMAR²³ and the metastatic oral SCC cell line OSC-19. The OSC-19 cell line was obtained from the laboratory of Faye Johnson, MD, PhD (M. D. Anderson). This cell line was established in Japan with cells from a patient with a well-differentiated SCCOT that metastasized to a cervical lymph node.²⁴ The OSC-19 and JMAR cells were retrovirally infected with the green fluorescent protein (GFP) and the luciferase gene. For construction of the retroviral luciferase vector (*Luc*), a polymerase chain reaction product of luciferase complementary DNA was amplified from the pGL3 vector (Promega Corp, Madison, Wisconsin) and cloned into pBMN-I-GFP (provided by Garry P. Nolan, PhD, Stanford University, Stanford, California) to generate the pBMN-I-Luc-GFP. The pBMN-I-Luc-GFP vector was transfected into Phoenix cells to generate a *Luc*-expressing retrovirus that was subsequently used to infect OSC-19 and JMAR cells. *Luc*-transduced stable OSC-19 and JMAR cells were obtained by sorting GFP-positive cells for green fluorescence by FACScan (Becton Dickinson, Franklin Lakes, New Jersey). All cell lines were grown in vitro in Dulbecco modified Eagle medium supplemented with 10% fetal bovine serum, L-glutamine, sodium pyruvate, nonessential amino acids, and a 2-fold vitamin solution (Life Technologies Inc, Grand Island, New York). Adherent monolayer cultures were maintained on plastic and incubated at 37°C in 5% carbon dioxide and 95% air. The cultures were free of *Mycoplasma* species and were maintained for no longer than 12 weeks after recovery from frozen stocks.

REAGENTS

The monoclonal rat antimouse VEGFR-2 antibody DC101 was provided by ImClone Systems Inc (New York, New York).²⁵ For in vivo administration, DC101 was provided undiluted at a concentration of 6.53 mg/mL and cetuximab (ImClone Systems Inc) was provided undiluted at a concentration of 2 mg/mL. Previous studies have shown that nonspecific IgG antibody developed in a similar fashion had no effect on tumor growth, similar to the effect of solvent, phosphate-buffered saline.²⁵ The following antibodies were purchased for immunohistochemi-

cal analysis: rabbit polyclonal anti-EGFR and anti-VEGFR-2 (Santa Cruz Biotechnology Inc, Santa Cruz, California), rabbit polyclonal anti-phospho-VEGFR-2 (pVEGFR-2; Oncogene, Cambridge, Massachusetts), rabbit polyclonal anti-phospho-EGFR (pEGFR; BioSource International, Camarillo, California), mouse anti-proliferating cell nuclear antigen (PCNA) clone PC-10 (DAKO A/S, Copenhagen, Denmark), rat monoclonal anti-CD31/platelet/endothelial cell adhesion molecule 1 (CD31/PECAM-1) (PharMingen, San Diego, California), peroxidase-conjugated goat antirabbit IgG (Jackson ImmunoResearch Laboratories, West Grove, Pennsylvania), peroxidase-conjugated rat antimouse IgG2a (Serotec; Harlan Bioproducts for Science Inc, Indianapolis, Indiana), peroxidase-conjugated goat antirat IgG1 (Jackson Research Laboratories), and Alexa Fluor 594-conjugated goat antirat IgG and Alexa Fluor 488-conjugated antirabbit IgG (Molecular Probes, Eugene, Oregon).

ESTABLISHMENT OF AN ORTHOTOPIC NUDE MOUSE MODEL OF SCCOT

OSC-19-Luc, OSC-19, and JMAR-Luc cells were harvested from subconfluent cultures by trypsinization and washed. The orthotopic nude mouse model of SCCOT was established by injecting OSC-19-Luc (3×10^4), OSC-19 (3×10^4), or JMAR-Luc (1×10^5) cells suspended in 30 μ L of serum-free Dulbecco modified Eagle medium into the mouse tongue as described previously.²⁶ Eleven to 13 days after the injection of SCCOT cells, when tumors were already established, mice with tumors of similar size and approximately equivalent tumor bioluminescence were randomized into 4 groups according to treatment (6-9 mice per group): placebo control, cetuximab alone, DC101 alone, and DC101 plus cetuximab. Drugs were administered intraperitoneally twice a week in the following doses: (1) 500 μ L of phosphate-buffered saline (placebo control), (2) 800 μ g of DC101, (3) 1 mg of cetuximab, and (4) 800 μ g of DC101 plus 1 mg of cetuximab. The mice were treated for 4 weeks. They were examined twice a week for weight loss and were killed by carbon dioxide asphyxiation if they lost more than 20% of their preinjection body weight or became moribund. The remaining mice were killed at 28 days after treatment. Necropsy was performed on the mice, with removal of tongue tumors and cervical lymph nodes. Half of the tumors were fixed in formalin and embedded in paraffin for immunohistochemical analysis and hematoxylin-eosin staining. The other half were embedded in optimal cutting temperature compound (Miles Inc, Elkhart, Indiana), rapidly frozen in liquid nitrogen, and stored at -80°C . The cervical lymph nodes were also embedded in paraffin and sectioned, stained with hematoxylin-eosin, and evaluated for the presence of metastases.

At the time of the necropsy, the tumor sizes were measured with microcalipers. Tumor volume (V) was calculated using the formula

$$V = (A)(B^2)\pi/6,$$

where A is the longest dimension of the tumor and B is the dimension of the tumor perpendicular to A. The percentage of tumor inhibition was calculated using the formula

$$(1 - [T/C]) \times 100,$$

where T and C represent the mean tumor volumes of the treatment group and the control group, respectively.

IMAGING OF ORTHOTOPIC TUMORS

Bioluminescence of the tongue tumors through standardized regions of interest was quantified using Living Images (Xeno-

gen Corp, Alameda, California). Animals were anesthetized with 2% isoflurane (Abbott, Abbott Park, Illinois) before and during imaging. An aqueous solution of luciferin (Xenogen Corp) at 150 mg/kg in a volume of 0.1 mL²⁷ was injected intraperitoneally 5 minutes prior to imaging. Animals were imaged at a peak time of 10 minutes after luciferin injection via a IVIS 200 imaging system (Xenogen Corp). The photons emitted from the luciferase-expressing cells within the animal were quantified using the software program Living Image (Xenogen, Corp) as an overlay on IGOR software (WaveMetrics, Portland, Oregon). The photon flux was calculated for each mouse using a rectangular region of interest encompassing the head and neck region of the mouse in a dorsal position. Animals were imaged after xenografting immediately (day 0) and on an almost weekly basis. Before use in vivo, engineered OSC-19-Luc and JMAR-Luc cells were confirmed in vitro to homogeneously express high levels of luciferase as monitored by the IVIS imaging system.

IMMUNOHISTOCHEMICAL AND IMMUNOFLOUORESCENT ANALYSIS

To examine the activity of the treatment, tumor specimens of 4 or more mice from each group were processed for routine histologic and immunohistochemical analyses. Paraffin-embedded tissues were prepared for detection of PCNA. Frozen tissues were used for detection of CD31/platelet-endothelial cell adhesion molecule (PECAM)-1 and TUNEL (terminal deoxynucleotidyl transferase-mediated dUTP [2'-deoxyuridine, 5'-triphosphate] nick-end labeling). Slides were prepared as previously described.²⁰ Immunostaining for PCNA (1:50) and CD31/PECAM-1 (1:400) was performed using the methods previously described.²⁰ The TUNEL staining assay was carried out using an apoptosis detection kit (Promega Corp). For CD31-TUNEL double staining, TUNEL staining was completed on slides already labeled with anti-CD31 antibody, as previously described.²⁰ Double staining for CD31/EGFR (1:200), CD31/activated-EGFR (1:50), CD31/VEGFR-2 (1:200), and CD31/activated VEGFR-2 (1:200) was performed as previously described.²⁰ Immunofluorescence microscopy was carried out using a Leica DMLA microscope (Leica Microsystems, Bannockburn, Illinois) equipped with a 100-W HBO mercury bulb and filter set (Chroma Inc, Brattleboro, Vermont) to individually capture red and blue fluorescent images. Images were captured using a cooled charged-coupled device Hamamatsu 5810 camera (Hamamatsu Corp, Bridgewater, New Jersey) and ImagePro Plus 6.0 software (Media Cybernetics, Bethesda, Maryland). Images at the stained sections were produced in the same microscope equipped with a 3-chip charged-coupled device color video camera (model DXC990; Sony Corp, Tokyo, Japan). Photomontages were prepared using Adobe Photoshop software (Adobe Systems Inc, San Jose, California). Photomontages were printed on a Sony digital color printer (model UP-D7000; Sony Corp).

QUANTIFICATION OF PCNA, MICROVESSEL DENSITY, APOPTOTIC TUMOR, AND ENDOTHELIAL CELLS

For the quantification analysis, 4 slides were prepared for each group, and 3 areas were selected on each slide. The percentage of stained cells among the total number of cells in each area and the mean proportion of stained cells in each group were calculated and compared. For quantification of TUNEL and PCNA expression, the positively stained cells were counted in 10 random 0.04-mm² fields at an original magnification of $\times 200$ per slide. To quantify microvessel density (MVD), areas containing

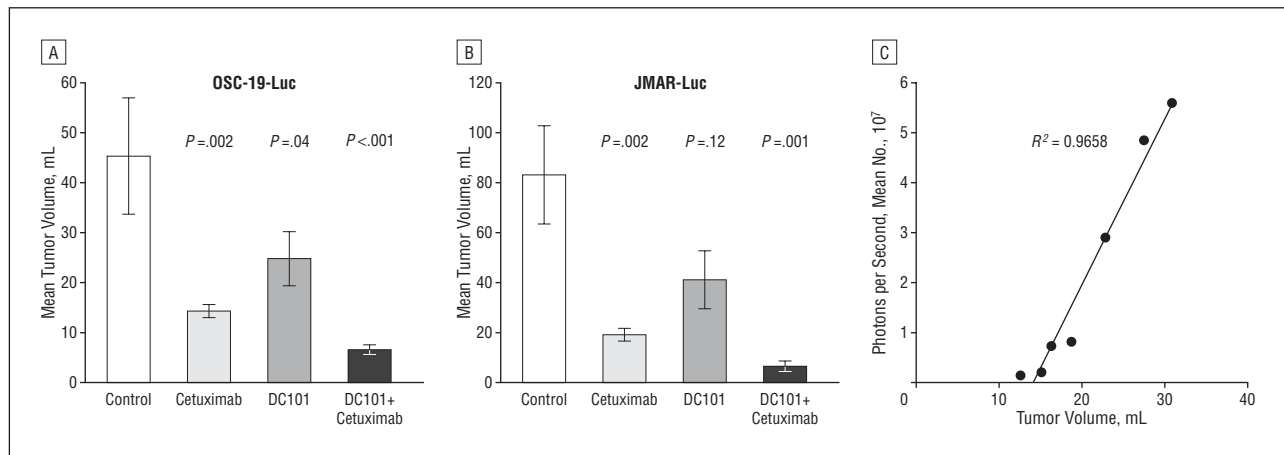


Figure 1. DC101, cetuximab, and combination therapy (DC101 plus cetuximab) inhibited the growth of squamous cell carcinoma of oral tongue xenografts in nude mice. A, OSC-19-Luc cells were injected into the tongues of nude mice. Eleven days later, mice were randomized and treated with placebo, DC101 (800 µg), cetuximab (1 mg), and DC101 (800 µg) plus cetuximab (1 mg), administered via intraperitoneal injection twice a week. Tumors were measured at the end of treatment (day 42). Error bars indicate SE. B, JMAR-Luc cells were injected into the tongues of nude mice. Eleven days later, mice were randomized and treated with placebo, DC101 (800 µg), cetuximab (1 mg), and DC101 (800 µg) plus cetuximab (1 mg), administered via intraperitoneal injection twice a week. Tumors were measured at the end of treatment. Error bars indicate SE. C, Linear correlation between mean number of photons per second as measured by the IVIS 200 imaging system (Xenogen Corp, Alameda, California) and tumor volume as measured by caliper.

higher numbers of tumor-associated blood vessels were identified at low microscopic power (original magnification, $\times 100$). Vessels completely stained with anti-CD31 antibodies were counted in 10 random 0.04-mm² fields at an original magnification of $\times 200$ per slide. Quantification of apoptotic endothelial cells was expressed as the mean of the ratios of apoptotic endothelial cells to the total number of endothelial cells in 10 random 0.04-mm² fields at an original magnification of $\times 200$.

STATISTICAL ANALYSIS

The Wilcoxon rank sum test was used to compare the differences in mouse tumor volume, bioluminescence, and mouse weight between the control and treatment groups on each day, with a significance level of $P < .01$. Associations between treatment groups and incidence of neck lymph node metastases were analyzed using the Fisher exact test. Survival was analyzed by the Kaplan-Meier method and compared with log-rank tests. The quantification of the immunohistochemical expression of MVD, TUNEL, PCNA, and CD31/TUNEL were compared using the Wilcoxon rank sum test, with a significance level of $P < .01$.

RESULTS

INHIBITION OF TUMOR GROWTH

As shown in **Figure 1** A and B, at the end of treatment day 42, there was a significant decrease in the size of tumors treated with DC101 plus cetuximab and with cetuximab alone compared with tumors injected with placebo ($P < .001$ and $P = .002$, respectively). The mean tumor volume of mice treated with DC101 alone was also lower than that of mice in the control group, but the difference was not statistically significant ($P = .04$). DC101 alone, cetuximab alone, and the combination treatment led to 45%, 68%, and 84% decreases, respectively, in the tumor volumes of the xenografts in the nude mouse models of SCCOT generated with an OSC-19-Luc cell line. We also confirmed the antitumor effect of these treatments in the orthotopic nude mouse model of SCCOT

generated by the OSC-19 and JMAR-Luc cell lines. The combination of DC101 and cetuximab produced significant inhibition of tumor growth in orthotopically implanted OSC-19 and JMAR-Luc cells as shown **Figure 1** B (data not shown).

REDUCTION OF BIOLUMINESCENCE IN ORTHOTOPIC SCCOT TUMORS

To see the effects of the treatment, we monitored the bioluminescence intensity of OSC-19-Luc cells. Prior to this, a pilot experiment was performed with 8 untreated mice to optimize the system and to establish the relationship between tumor volume and mean number of photons per second. At the end of the experiment, the 7 remaining mice were imaged and killed on the same day, and their tongue tumors were excised. **Figure 1** C shows the relationship between mean number of photons per second and tumor volume (as measured by calipers). The results show that photons per second are a relative measure of tumor volume in our SCCOT orthotopic nude mice in this system. As shown in **Figure 2** A, in this bioluminescence imaging system, a significant reduction of bioluminescence was detected at the end of treatment (day 42) in the mice treated with DC101 plus cetuximab (mean light reduction, 97% [$P < .001$]). The mean bioluminescence intensities of the mice in the DC101 group and the cetuximab group were also lower than those of mice in the control group; however, the differences were not statistically significant (mean light reduction, 62% [$P = .09$] and 83% [$P = .02$], respectively). A significant reduction of bioluminescence was detected on the final day.

Similarly, these antitumor effects of cetuximab alone and DC101 alone were also observed in the JMAR-Luc orthotopic model (**Figure 2** B). Bioluminescence intensity was lower in the combination treatment group than in the control group at all points; however, the difference did not reach significance. Each therapy was well tolerated by the animals without significant adverse ef-

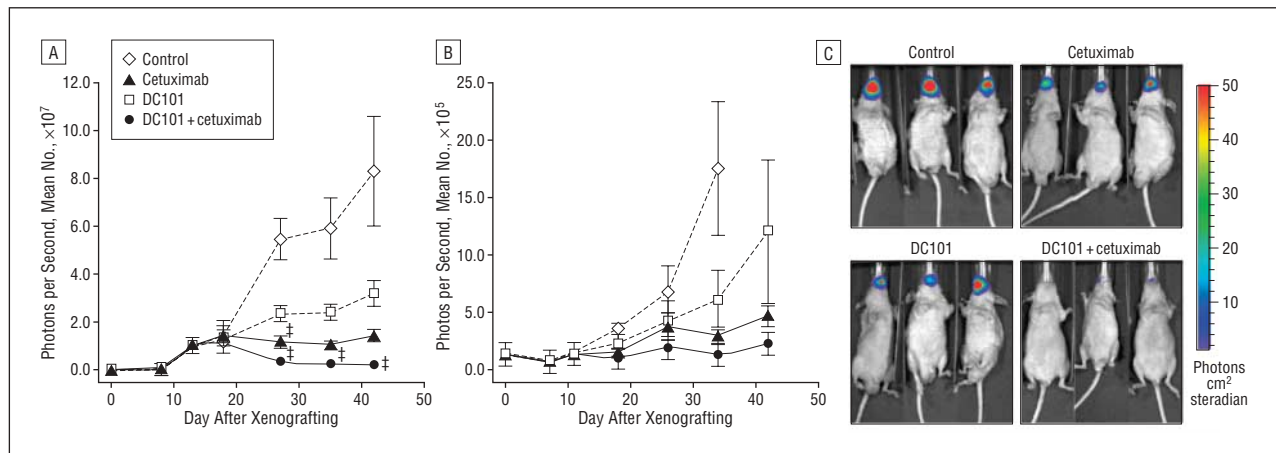


Figure 2. The antitumor effects of combination epidermal growth factor receptor plus vascular endothelial growth factor receptor 2 targeted therapy against squamous cell carcinoma of the oral tongue xenograft mouse model monitored by bioluminescence imaging. A, The effects of treatment on OSC-19-Luc orthotopic tumor were followed by bioluminescence imaging. Data points represent the mean (cm=8-9 animals per group); error bars indicate SE. $P < .05$ compared with the control group by the Wilcoxon rank sum test. B, The effects of treatment on JMAR-Luc orthotopic tumor were followed by bioluminescence imaging. Data points represent the mean (6 animals per group); error bars indicate SE. $P < .05$ compared with the control group by the Wilcoxon rank sum test. Photon counts were calculated from the imaging data using the IVIS Living Image software (Xenogen Corp, Alameda, California). C, Representative bioluminescence images corresponding to OSC-19-Luc tumors from each treatment group at the end of the study (day 42).

fects, as determined by the maintenance of body weight (data not shown).

IMPROVEMENT IN SURVIVAL

Animals injected with JMAR-Luc cells were kept alive until they met some or all criteria for carbon dioxide asphyxiation (ie, large tumor volume, significant weight loss, hunched posture, and ruffled coat). All of the mice in the control group in the survival study met the criteria for carbon dioxide asphyxiation by day 35, mostly due to weight loss. The median survival periods for the control, DC101, cetuximab, and combination treatment groups were 28, 42, 40, and 42 days, respectively. The differences in survival between the groups were statistically significant by log-rank test ($P < .001$). All treatment group animals survived longer than the control group animals. No significant difference was found between the cetuximab and combination treatment groups; however, both of these groups appeared to have the longest survivals without any deaths. When compared with animals treated with DC101 alone, however, the differences in survival durations did not reach statistical significance (**Figure 3** and **Table 1**).

DECREASED INCIDENCE OF CERVICAL LYMPH NODE METASTASES

In the groups of animals with OSC-19-Luc and OSC-19 tumors, cervical lymph nodes were harvested and examined histologically to identify cervical lymph node metastases. As shown in Figure 3 and Table 1, the cervical lymph node metastases were detected in 10 (63%) of the 16 control mice, 5 (31%) of the 16 cetuximab-treated mice, 5 (31%) of the 16 DC101-treated mice, and 1 (6%) of the 16 mice in the combination treatment group. Thus, combination treatment inhibited the development of cervical lymph node metastases markedly, and the differences in outcomes in the combination therapy and con-

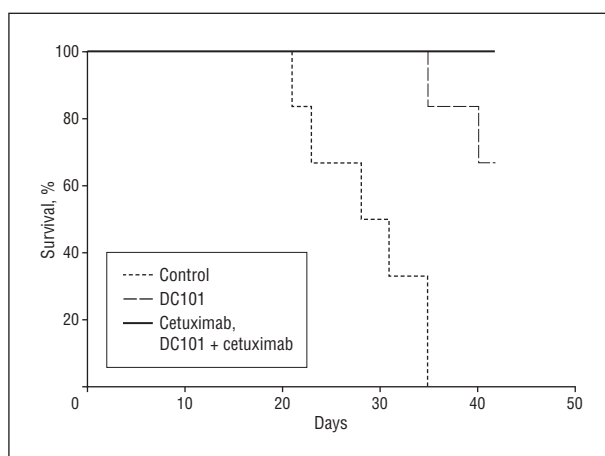


Figure 3. Kaplan-Meier survival curve showing the effects of epidermal growth factor receptor plus vascular endothelial growth factor receptor 2 targeted therapy on the survival of nude mice bearing orthotopic squamous cell carcinoma of the oral tongue xenografts. $P < .001$ for cetuximab and combination treatment groups when compared with the control group.

Table 1. Effects of Cetuximab and DC101 on the Incidence of Lymph Node Metastasis in Nude Mice Bearing Orthotopic SCCOT Xenografts

Treatment Groups	Mice With Cervical Lymph Node Metastasis, No. (%) (N=16)	P Value vs Control ^a
Placebo	10 (63)	
Cetuximab	5 (31)	.07
DC101	5 (31)	.07
DC101 + cetuximab	1 (6)	.003

Abbreviation: SCCOT, squamous cell carcinoma of the oral tongue.

^aThe combination treatment inhibited the incidence of cervical lymph node metastases markedly, with only 1 mouse, and the difference between combination treatment group and the control group was significant ($P = .003$). Although there were no significant differences, treatment with DC101 plus cetuximab resulted in a lower rate of locoregional metastases compared with the other treatment groups ($P = .07$ for both the cetuximab and DC101 groups).

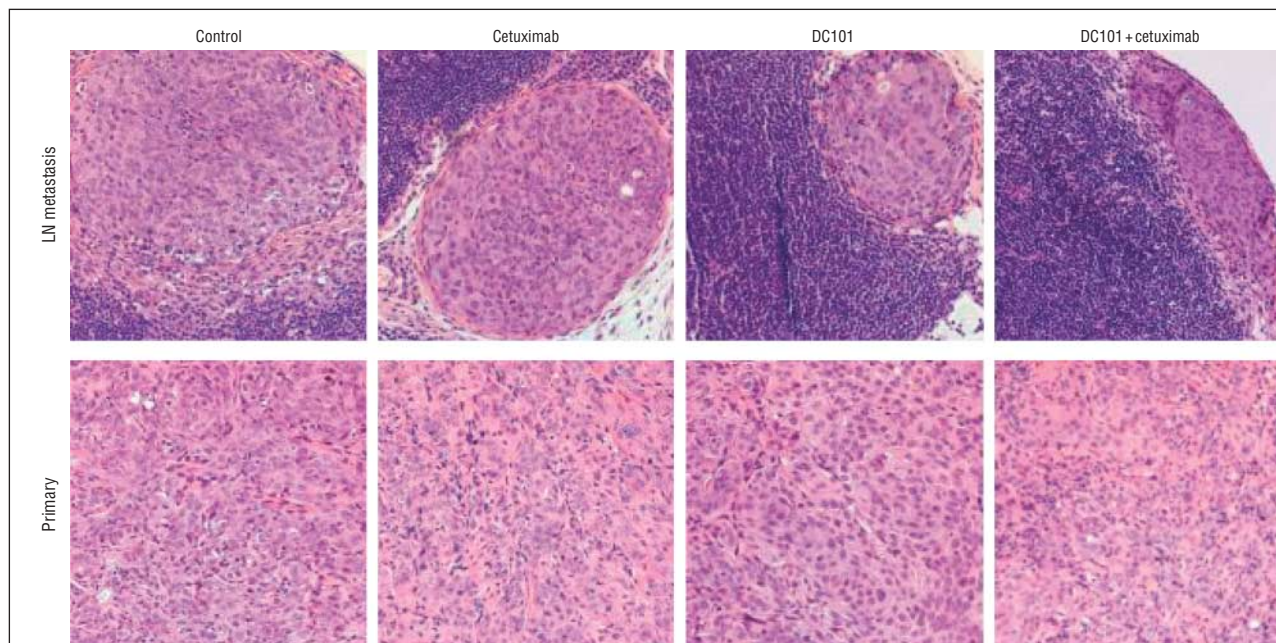


Figure 4. Cervical lymph node (LN) of squamous cell carcinoma of the oral tongue xenografts with subcapsular metastasis.

control groups were significant ($P = .003$). The difference in metastasis in the control group and that in the DC101 and cetuximab groups did not reach statistical significance (**Figure 4**). The difference in metastasis in the combination treatment group and the DC101 and cetuximab groups also did not reach statistical significance. In the groups of animals with JMAR-Luc tumors, only 1 neck lymph node metastasis was found in the group treated with DC101 (data not shown).

ANTIANGIOGENIC EFFECTS OF COMBINED TREATMENT WITH DC101 AND CETUXIMAB

To clarify the mechanism of the antiangiogenic effects of DC101 and cetuximab, we stained tumor sections for CD31-specific antibodies and determined the MVD by the number of CD31-positive microvessels (**Figure 5**). OSC-19 cells were injected into the tongues of nude mice. Eleven days later, mice were randomized and treatment was started with placebo, DC101 (800 μ g), cetuximab (1 mg), or DC101 (800 μ g) plus cetuximab (1 mg). Mice were killed after 14 days of treatment. Primary tumors were harvested and stained with specific antibodies. As given in **Table 2**, the MVD was highest in the control group. The tumors of mice treated with DC101 and with DC101 in combination with cetuximab showed significantly lower MVDs compared with controls (41% and 64%, respectively [$P < .01$]). Treatment with cetuximab decreased MVD by 30%; however, the difference compared with that of the control group was not significant. To examine *in vivo* cell proliferation and apoptosis, antibodies were used against PCNA and the TUNEL assay, respectively. Cells positive for PCNA were abundant in the control group and decreased in treated tumors (Figure 5). As given in Table 2, the mean (SD) percentage of PCNA-positive tumor cells in the control group was 73.9 (9.3). Compared with the controls, signifi-

cantly lower percentages of PCNA-positive tumor cells ($P < .01$) were detected in the DC101 group (58.3 [12.7]), the cetuximab group (53.4 [11.0]), and the DC101 plus cetuximab group (41.0 [10.6]). Although TUNEL-positive cells were rarely detected in tumors from the control mice, a progressive increase in the green fluorescent apoptotic cells was found in the tumors from the treated mice (Figure 5). The percentage of TUNEL-positive cells in the control group was 1.6 (0.1). Compared with the controls, significantly higher percentages of TUNEL-positive tumor cells were detected in the DC101 group (8.7 [3.0]), cetuximab group (16.5 [9.1]), and DC101 plus cetuximab group (35.0 [13.4]) ($P < .01$; Table 2). Finally, double staining for CD31 (red staining)/TUNEL (green staining) revealed that the percentage of apoptotic endothelial cells (yellow staining) was significantly higher in the tumors of mice treated with cetuximab alone, DC101 alone, and DC101 plus cetuximab than in the control group (Table 2 and Figure 5 [$P < .01$]).

INHIBITION OF EGFR AND VEGFR-2 PHOSPHORYLATION WITH DC101 PLUS CETUXIMAB

To determine whether treatment with DC101 plus cetuximab inhibits phosphorylation of the targeted receptors EGFR and VEGFR-2, double staining for CD31/activated EGFR and CD31/EGFR, which was done with CD31 (red staining)/total EGFR and activated EGFR (green staining) and CD31/total VEGFR-2 and activated VEGFR-2 (green staining), was performed. Tumors from the control group or the DC101 plus cetuximab group showed similar levels of EGFR expression (**Figure 6A**), whereas only tumors from control mice or mice treated with DC101 stained positive for phosphorylated EGFR, a finding consistent with inhibition of EGFR autophosphorylation *in vivo*.

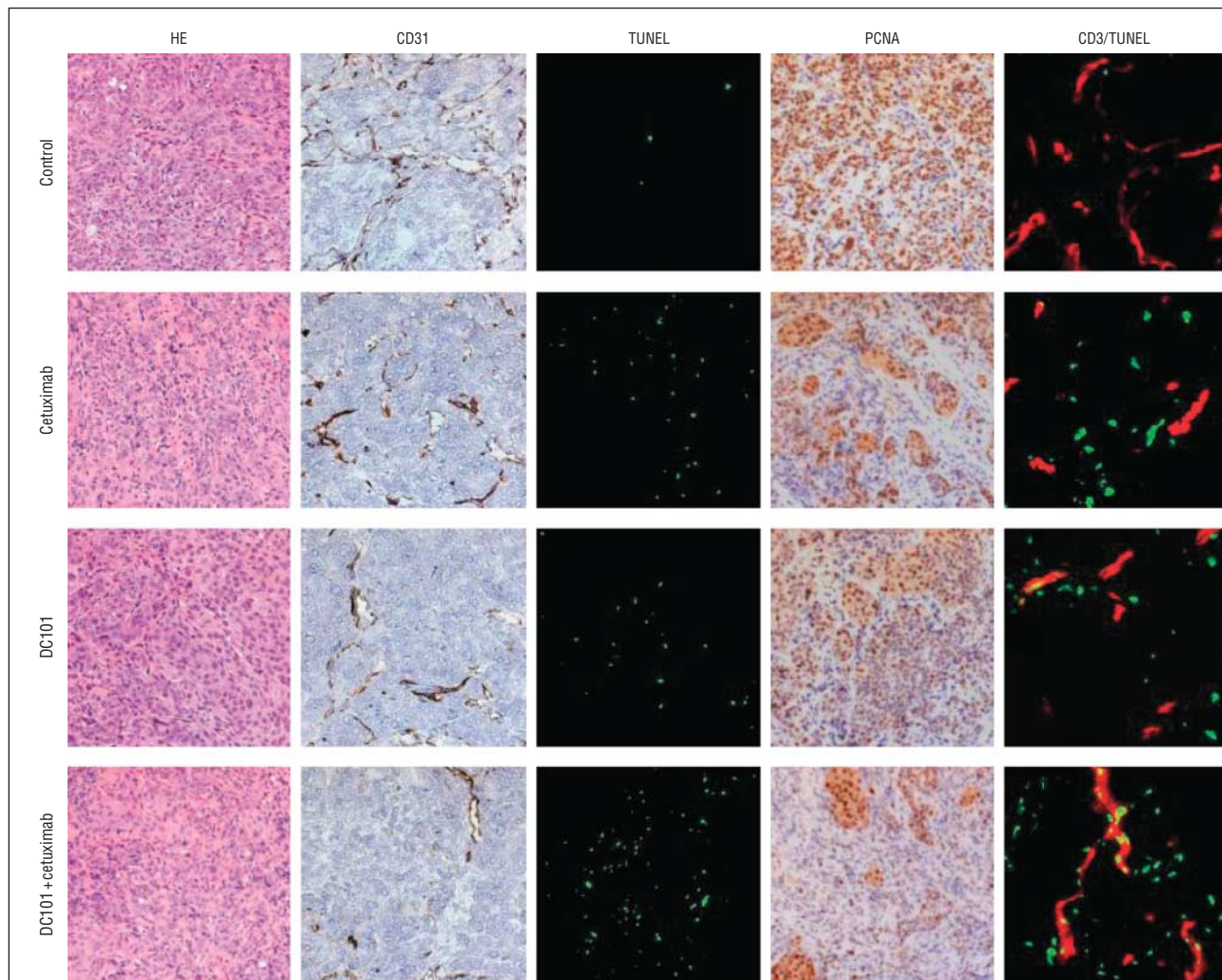


Figure 5. Immunohistochemical analyses of OSC-19 tumors in nude mouse xenografts. Tumors were harvested after 14 days of treatment, and representative sections obtained from OSC-19 tumors were stained for hematoxylin-eosin (HE) and immunostained for expression of CD31 (endothelial cell marker), proliferating cell nuclear antigen (PCNA) (tumor cell proliferation), and TUNEL (terminal deoxynucleotidyl transferase-mediated dUTP [2'-deoxyuridine, 5'-triphosphate] nick-end labeling) (tumor cell apoptosis) (original magnification $\times 100$). Double staining for CD31 (red)/TUNEL (green) was also performed to reveal induction of apoptosis in tumor-associated endothelial cells; apoptotic endothelial cells were identified as a merge of red and green fluorescence (original magnification $\times 200$).

Table 2. Quantitative Immunohistochemical Analysis of OSC-19 Tumors in the Tongues of Nude Mice

Variable	Treatment Group			
	Control	Cetuximab	DC101	DC101 + Cetuximab
Tumor cells, mean (SD), %				
TUNEL ^a	1.6 (0.1)	16.5 (9.1) ^d	8.7 (3.0) ^d	35.0 (13.4) ^d
PCNA ^a	73.9 (9.3)	53.4 (11.0) ^d	58.3 (12.7) ^d	41.0 (10.6) ^d
Endothelial cells, mean (SD)				
MVD ^b	38.2 (9.9)	26.9 (4.2)	22.5 (7.3) ^d	13.9 (5.5) ^d
CD31/TUNEL, % ^c	0.3 (0.3)	6.1 (2.0) ^d	15.1 (7.8) ^d	24.9 (10.8) ^d

Abbreviations: MVD, microvessel density; PCNA, proliferating cell nuclear antigen; TUNEL, terminal deoxynucleotidyl transferase-mediated dUTP (2'-deoxyuridine, 5'-triphosphate) nick-end labeling.

^aPositivity for PCNA and TUNEL was quantitated as the percentage of positively stained cells to total cells in 10 random 0.04-mm² fields at an original magnification of $\times 200$ per slide.

^bMicrovessel density was determined by measuring the number of completely stained blood vessels in 10 random 0.159-mm² fields at an original magnification of $\times 100$ per slide.

^cPositivity for CD31/TUNEL was quantitated as the percentage of CD31/TUNEL-positive cells to total endothelial cells in 10 random 0.04-mm² fields at an original magnification of $\times 200$ per slide.

^d $P < .01$ compared with controls.

In addition, the status of EGFR activation in endothelial cells (double staining: yellow) was also significantly suppressed in OSC-19 tumors of mice treated

with DC101 plus cetuximab (Figure 6B). The level of expression of VEGFR-2 on endothelial cells showed double staining (yellow) of fluorescent CD31 staining

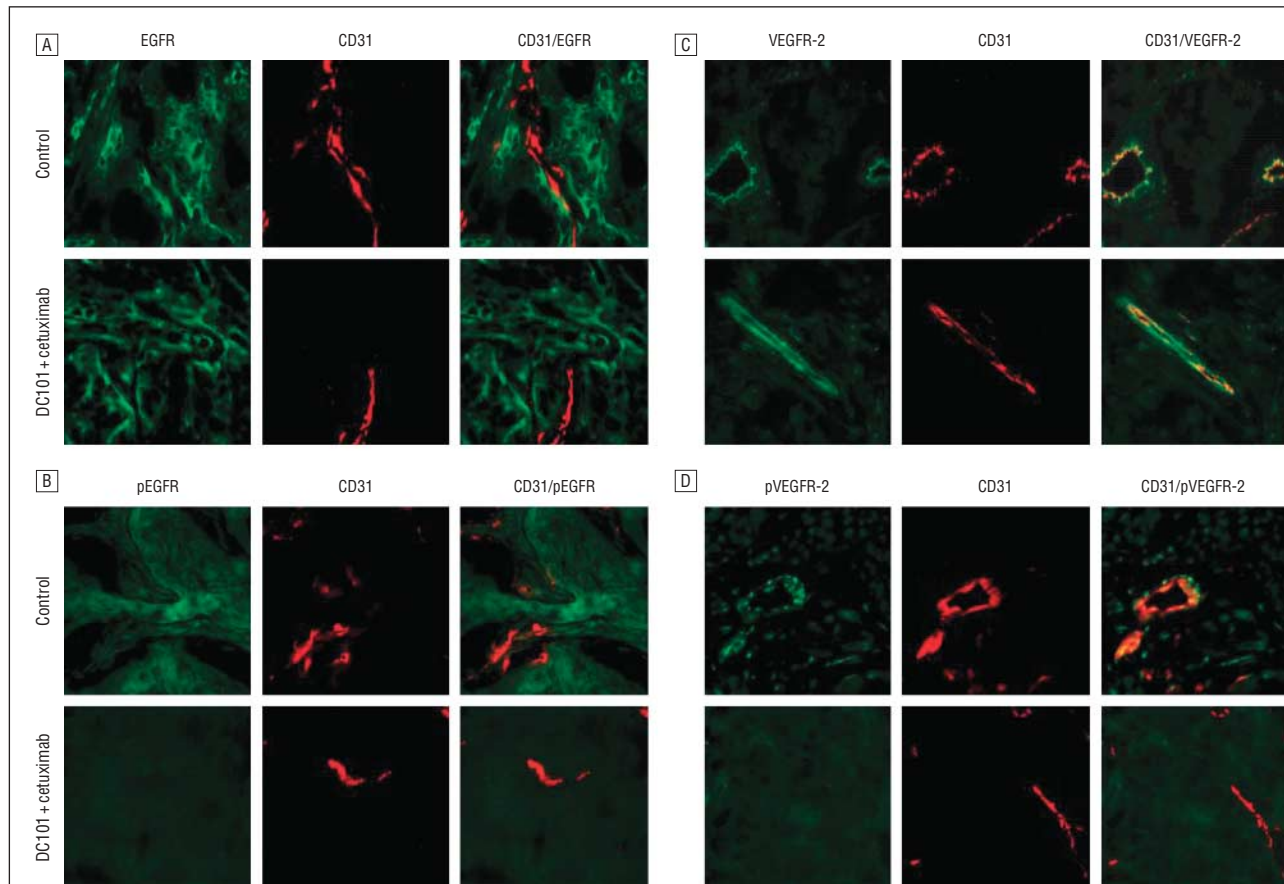


Figure 6. Double immunofluorescent staining of OSC-19 tumors in nude mouse xenografts. Tumors were harvested from the control group or from the DC101 plus cetuximab group. The sections were immunostained for expression of CD31 (endothelial cells marker, red)/epidermal growth factor receptor (EGFR) (A), CD31/activated EGFR (pEGFR) (B), CD31/vascular endothelial growth factor receptor 2 (VEGFR-2) (C), and CD31/activated VEGFR-2 (pVEGFR-2) (D) (original magnification $\times 200$).

(red) specific for endothelial cells with fluorescent green staining of VEGFR-2 and did not vary significantly among the tumor and endothelial cells from mice in all 4 treatment groups (Figure 6C); however, treatment with the combination of DC101 plus cetuximab decreased double staining (yellow) for these markers, a finding consistent with reduced signaling through VEGFR-2 in tumor-associated endothelial cells (Figure 6D).

COMMENT

In this study, we found that blockade of the EGFR and VEGFR-2 pathways by DC101 and cetuximab inhibits not only orthotopic tumor growth of SCCOT but also the incidence of cervical lymph node metastases in nude mice. Our data also demonstrated that the combination of DC101 and cetuximab prolonged survival and led to a significant suppression of proliferation, vascularity, and phosphorylation of these 2 receptors in vivo and a significant enhancement of apoptotic cells in both tumor and endothelial cells in our SCCOT orthotopic nude mouse model.

The presence of cervical lymph node metastasis is a critical event for patients with SCCOT because this is the most accurate predictor of poor treatment outcome. More than 30% of patients with SCCOT can be expected to have

cervical lymph node metastases, even if abnormal lymph node metastases are not detected clinically.²⁸ The best way to manage cervical lymph node metastases remains controversial, and we cannot always predict cervical lymph node metastasis from the size and extent of invasion of the primary tumors. Therefore, the development of effective therapies in metastatic SCCOT is required. We developed an orthotopic nude mouse model of SCCOT by injecting metastatic SCCOT cells (OSC-19 and OSC-19-Luc) and invasive SCCOT cells (JMAR-Luc) into the tongues of athymic mice. Our SCCOT mouse model follows the metastatic pattern of human tumors that we have reported previously.²⁶ Using this tongue tumor model, we were able to evaluate the effect of targeted systemic agents on cervical lymph node metastases.

We also showed that combination treatment with DC101 plus cetuximab inhibits tumor growth of OSC-19-Luc cells and JMAR-Luc cells compared with the placebo control in vivo. This finding is consistent with reports of this treatment in other preclinical models^{5,29} and with our reports that treatment of SCCOT with small-molecule tyrosine kinase inhibitors inhibited EGFR and VEGFR-2 signaling in our SCCOT orthotopic model.²⁰

Combination treatment inhibited the development of cervical lymph node metastasis in the orthotopic nude mouse model. Our findings are consistent with a study

that reported an inhibitory effect of DC101 plus paclitaxel on metastasis of bladder cancer.³⁰ The process of metastasis is complex, and the genetic and biochemical determinants remain incompletely understood in most cancers, including SCCOT. However, angiogenesis is thought to play an important role in the proliferation of primary tumors by maintaining a supply of oxygen and nutrients that support tumor growth and metastasis.³¹ However, the EGFR signaling pathway is one of the major pathways regulating tumor proliferation, which is required at the secondary site to establish metastasis. Several prior studies have reported that overexpression of VEGF, which plays a major role in angiogenesis, is associated with poor prognosis and metastases in SCCOT.⁷⁻¹⁰ In addition, EGFR overexpression is a strong predictor of decreased survival in SCCHN.¹⁹ Moreover, the VEGF and EGFR pathways seem to be closely related, particularly with respect to angiogenesis in many tumors. The EGFR pathway increases angiogenesis by upregulating VEGF or other key mediators in the angiogenic process,³² and EGFR blockade results in the downregulation of proangiogenic mediators in preclinical models.³³ In the present study, combination treatment with DC101 plus cetuximab potentially inhibited the phosphorylation of these 3 receptors, significantly induced both endothelial and tumor apoptosis, and decreased tumor MVD and proliferation in OSC-19 cells *in vivo*. These findings are consistent with other reports.^{20,29}

Lastly, the combination treatment significantly prolonged survival in the orthotopic nude mouse model of SCCOT. At the same time, treatment with cetuximab alone also showed a significant effect on the survival rate in the SCCOT model. According to this survival analysis and the inhibitory effect of tumor growth, it is possible that treatment with only cetuximab may be enough to treat our SCCOT model, whereas treatment with DC101 alone showed only limited antitumor effects. However, in our findings, cetuximab combined with blockade of VEGFR-2 signaling was very useful in preventing the incidence of cervical lymph node metastases. Treatment with DC101 alone showed an inhibitory effect on the incidence of cervical lymph node metastases, and the combination of cetuximab and DC101 showed marked inhibition, whereas the effect of cetuximab treatment against the incidence of cervical lymph node metastases did not reach significance.

On the basis of promising preclinical results, angiogenesis inhibitors such as bevacizumab, a humanized anti-VEGF antibody, and a small-molecule tyrosine kinase inhibitor of VEGFR-2 have been studied extensively in preclinical models and clinical trials, including SCCHN,³⁴ and cetuximab demonstrated a significant improvement in median overall survival compared with radiotherapy alone in a phase 3 trial against SCCHN.²¹ Clinical trials with EGFR and VEGFR-2 inhibitors, such as vandetanib, are also under way in the study of SCCHN.

In conclusion, targeted therapy combining the EGFR and VEGFR pathways with monoclonal antibodies showed significant antitumor activity against an orthotopic mouse model of SCCOT and also inhibited the incidence of cervical lymph node metastases *in vivo*. This treatment blocked the phosphorylation of

these receptors, inducing both endothelial apoptosis and tumor apoptosis and decreasing tumor MVD and proliferation. These results suggest that this combination treatment may be an effective strategy against metastatic SCCOT and warrants further preclinical trials.

Submitted for Publication: July 18, 2008; accepted October 15, 2008.

Correspondence: Jeffrey N. Myers, MD, PhD, Department of Head and Neck Surgery, Unit 441, The University of Texas M. D. Anderson Cancer Center, 1515 Holcombe Blvd, Houston, TX 77030-4009 (jmyers@mdanderson.org).

Author Contributions: All authors had full access to all the data in the study and take responsibility for the integrity of the data and the accuracy of the data analysis. *Study concept and design:* Sano, Zhu, and Myers. *Acquisition of data:* Sano, Choi, Milas, Zhou, Galer, Su, Gule, and Zhao. *Analysis and interpretation of data:* Sano and Myers. *Drafting of the manuscript:* Sano. *Critical revision of the manuscript for important intellectual content:* Choi, Milas, Zhou, Galer, Su, Gule, Zhao, Zhu, and Myers. *Statistical analysis:* Sano. *Obtained funding:* Myers. *Administrative, technical, and material support:* Zhu and Myers. *Study supervision:* Myers.

Financial Disclosure: Dr Zhu is an employee of ImClone Systems Inc.

Funding/Support: This work was supported by grant P50 CA097007A from the M. D. Anderson Cancer Center SPORE in Head and Neck Cancer; The University of Texas M. D. Anderson Cancer Center PANTHEON Program; award number T32CA060374 from the National Cancer Institute; and support grant CA16672 from the NIH Cancer Center. ImClone Systems Inc provided the DC101 and cetuximab used in the study.

Previous Presentation: This study was presented at the Seventh International Conference on Head and Neck Cancer of the American Head and Neck Society; July 21, 2008; San Francisco, California.

Additional Contributions: Carol M. Johnston provided technical assistance with the immunohistochemical staining, and Vickie J. Williams provided a critical editorial review of the manuscript.

REFERENCES

1. Jemal A, Siegel R, Ward E, Murray T, Xu J, Thun MJ. Cancer statistics, 2007. *CA Cancer J Clin.* 2007;57(1):43-66.
2. Silverman S Jr. Demographics and occurrence of oral and pharyngeal cancers. The outcomes, the trends, the challenge. *J Am Dent Assoc.* 2001;132(suppl):7S-11S.
3. Grandi C, Alloisio M, Moglia D, et al. Prognostic significance of lymphatic spread in head and neck carcinomas: therapeutic implications. *Head Neck Surg.* 1985; 8(2):67-73.
4. Baselga J. Targeting tyrosine kinases in cancer: the second wave. *Science.* 2006; 312(5777):1175-1178.
5. Tonra JR, Deevi DS, Corcoran E, et al. Synergistic antitumor effects of combined epidermal growth factor receptor and vascular endothelial growth factor receptor-2 targeted therapy. *Clin Cancer Res.* 2006;12(7, pt 1):2197-2207.
6. Jain RK. Molecular regulation of vessel maturation. *Nat Med.* 2003;9(6):685-693.
7. Smith BD, Smith GL, Carter D, Sasaki CT, Haffty BG. Prognostic significance of vascular endothelial growth factor protein levels in oral and oropharyngeal squamous cell carcinoma. *J Clin Oncol.* 2000;18(10):2046-2052.

8. Kishimoto K, Sasaki A, Yoshihama Y, Mese H, Tsukamoto G, Matsumura T. Expression of vascular endothelial growth factor-C predicts regional lymph node metastasis in early oral squamous cell carcinoma. *Oral Oncol.* 2003;39(4):391-396.
9. Uehara M, Sano K, Ikeda H, et al. Expression of vascular endothelial growth factor and prognosis of oral squamous cell carcinoma. *Oral Oncol.* 2004;40(3):321-325.
10. Tanigaki Y, Nagashima Y, Kitamura Y, Matsuda H, Mikami Y, Tsukuda M. The expression of vascular endothelial growth factor-A and -C, and receptors 1 and 3: correlation with lymph node metastasis and prognosis in tongue squamous cell carcinoma. *Int J Mol Med.* 2004;14(3):389-395.
11. Neuchrist C, Erovic BM, Handisurya A, et al. Vascular endothelial growth factor receptor 2 (VEGFR2) expression in squamous cell carcinomas of the head and neck. *Laryngoscope.* 2001;111(10):1834-1841.
12. Ullrich A, Schlessinger J. Signal transduction by receptors with tyrosine kinase activity. *Cell.* 1990;61(2):203-212.
13. El-Rayes BF, LoRusso PM. Targeting the epidermal growth factor receptor. *Br J Cancer.* 2004;91(3):418-424.
14. Khazaie K, Schirrmacher V, Lichtner RB. EGF receptor in neoplasia and metastasis. *Cancer Metastasis Rev.* 1993;12(3-4):255-274.
15. Bruns CJ, Harbison MT, Davis DW, et al. Epidermal growth factor receptor blockade with C225 plus gemcitabine results in regression of human pancreatic carcinoma growing orthotopically in nude mice by antiangiogenic mechanisms. *Clin Cancer Res.* 2000;6(5):1936-1948.
16. Overholser JP, Prewett MC, Hooper AT, Waksal HW, Hicklin DJ. Epidermal growth factor receptor blockade by antibody IMC-C225 inhibits growth of a human pancreatic carcinoma xenograft in nude mice. *Cancer.* 2000;89(1):74-82.
17. Prewett MC, Hooper AT, Bassi R, Ellis LM, Waksal HW, Hicklin DJ. Enhanced antitumor activity of anti-epidermal growth factor receptor monoclonal antibody IMC-C225 in combination with irinotecan (CPT-11) against human colorectal tumor xenografts. *Clin Cancer Res.* 2002;8(5):994-1003.
18. Xia W, Lau YK, Zhang HZ, et al. Combination of EGFR, HER-2/neu, and HER-3 is a stronger predictor for the outcome of oral squamous cell carcinoma than any individual family members. *Clin Cancer Res.* 1999;5(12):4164-4174.
19. Ulanovski D, Stern Y, Roizman P, Shpitzer T, Popovtzer A, Feinmesser R. Expression of EGFR and Cerb-B2 as prognostic factors in cancer of the tongue. *Oral Oncol.* 2004;40(5):532-537.
20. Yigitbasi OG, Younes MN, Doan D, et al. Tumor cell and endothelial cell therapy of oral cancer by dual tyrosine kinase receptor blockade. *Cancer Res.* 2004;64(21):7977-7984.
21. Bonner JA, Harari PM, Giralt J, et al. Radiotherapy plus cetuximab for squamous-cell carcinoma of the head and neck. *N Engl J Med.* 2006;354(6):567-578.
22. Herbst RS, Johnson DH, Mininberg E, et al. Phase I/II trial evaluating the anti-vascular endothelial growth factor monoclonal antibody bevacizumab in combination with the HER-1/epidermal growth factor receptor tyrosine kinase inhibitor erlotinib for patients with recurrent non-small-cell lung cancer. *J Clin Oncol.* 2005;23(11):2544-2555.
23. Swan EA, Jasser SA, Holsinger FC, Doan D, Bucana C, Myers JN. Acquisition of anoikis resistance is a critical step in the progression of oral tongue cancer. *Oral Oncol.* 2003;39(7):648-655.
24. Yokoi T, Yamaguchi A, Odajima T, Furukawa K. Establishment and characterization of a human cell line derived from a squamous cell carcinoma of the tongue. *Tumor Res.* 1988;23:43-57.
25. Prewett M, Huber J, Li Y, et al. Antivascular endothelial growth factor receptor (fetal liver kinase 1) monoclonal antibody inhibits tumor angiogenesis and growth of several mouse and human tumors. *Cancer Res.* 1999;59(20):5209-5218.
26. Myers JN, Holsinger FC, Jasser SA, Bekele BN, Fidler IJ. An orthotopic nude mouse model of oral tongue squamous cell carcinoma. *Clin Cancer Res.* 2002;8(1):293-298.
27. Jenkins DE, Yu SF, Hornig YS, Purchio T, Contag PR. In vivo monitoring of tumor relapse and metastasis using bioluminescent PC-3M-luc-C6 cells in murine models of human prostate cancer. *Clin Exp Metastasis.* 2003;20(8):745-756.
28. Shah JP, Andersen PE. Evolving role of modifications in neck dissection for oral squamous carcinoma. *Br J Oral Maxillofac Surg.* 1995;33(1):3-8.
29. Jung YD, Mansfield PF, Akagi M, et al. Effects of combination anti-vascular endothelial growth factor receptor and anti-epidermal growth factor receptor therapies on the growth of gastric cancer in a nude mouse model. *Eur J Cancer.* 2002;38(8):1133-1140.
30. Inoue K, Slaton JW, Davis DW, et al. Treatment of human metastatic transitional cell carcinoma of the bladder in a murine model with the anti-vascular endothelial growth factor receptor monoclonal antibody DC101 and paclitaxel. *Clin Cancer Res.* 2000;6(7):2635-2643.
31. Kerbel RS. Tumor angiogenesis: past, present and the near future. *Carcinogenesis.* 2000;21(3):505-515.
32. Perrotte P, Matsumoto T, Inoue K, et al. Anti-epidermal growth factor receptor antibody C225 inhibits angiogenesis in human transitional cell carcinoma growing orthotopically in nude mice. *Clin Cancer Res.* 1999;5(2):257-265.
33. Ellis LM. Epidermal growth factor receptor in tumor angiogenesis. *Hematol Oncol Clin North Am.* 2004;18(5):1007-1021.
34. Savvides P, Greskovich J, Bokar J, et al. Phase II study of bevacizumab in combination with docetaxel and radiation in locally advanced squamous cell cancer of the head and neck (SCCHN) [abstract]. *J Clin Oncol.* 2007;25(18S):6068.